Available online at www.sciencedirect.com
SCIENCE DIRECT®
PERGAMON
Polyhedron 22 (2003) 1695–1699
POLYHEDRON
www.elsevier.com/locate/poly

Complexation and extractability studies of lanthanide elements by 2,2′-[1,2-phenylenebis(oxy)]-bis(*N*-methyl-*N*-phenyl(acetamide))

Yu-Liang Zhang [a], Wei-Hua Jiang [a], Wei-Sheng Liu [a,*], Yong-Hong Wen [a], Kai-Bei Yu [b]

[a] *College of Chemistry and Chemical Engineering, Lanzhou University, Lanzhou 730000, China*
[b] *Chengdu Center of Analysis and Measurement, Academia Sinica, Chengdu 610041, China*

Received 3 March 2003; accepted 25 April 2003

Abstract

Solid complexes of lanthanide picrates with 2,2′-[1,2-phenylenebis(oxy)]-bis(*N*-methyl-*N*-phenyl(acetamide)) (L) have been prepared and characterized by elemental analysis, conductivity measurements, IR, electronic and ^{1}H NMR spectroscopies. The crystal structure of terbium complex shows a nona-coordination polyhedron in the form of a distorted mono-capped square antiprism. The extractability of lanthanide ions by L has been investigated using multitracer technology.

Keywords: Lanthanide picrates complexes; X-ray structures; Solvent extraction

1. Introduction

Acyclic polyethers offer many advantages over the use of crown ethers in the extraction and analysis (ion-selective electrodes) of rare earth metals. Their ring-like coordination structures and terminal group effects on the extractability have been widely studied [1–5]. Ding et al. have reported that an amide acyclic polyether *N*,*N*,*N*′,*N*′-tetraphenyl-3,6-dioxaoctanediamide has a larger separation factor and distribution ratio to lighter lanthanide ions than that of dicyclohexyl-18-crown-6 ether. The picrate ion (pic^-) is often used as accompanying ion and enters the organic phase in the extraction. To investigate the effects of the skeleton and terminal group on the coordination property and extractability of lanthanide ions, we prepared another amide acyclic polyether 2,2′-[1,2-phenylenebis(oxy)]-bis(*N*-methyl-*N*-phenyl(acetamide)) (L) and its rare earth metal picrate complexes. The extractability by L for rare earth metal ions has also been discussed in consideration with the crystal structure

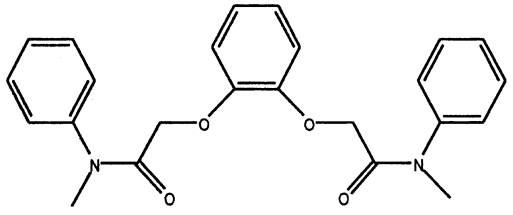

2,2′-[1,2-phenylenebis(oxy)]-bis(*N*-methyl-*N*-phenyl (acetamide) (L)

2. Experimental

2.1. Materials

Lanthanide picrates [6] and L [7] were prepared according to literature methods. All commercially available chemicals were of A.R. grade and were used without further purification.

* Corresponding author. Tel.: +86-931-891-2552; fax: +86-931-891-2582.
E-mail address: liuws@lzu.edu.cn (W.-S. Liu).

0277-5387/03/$ - see front matter
doi:10.1016/S0277-5387(03)00329-2

2.2. Preparation of the ligand (L)

Anhydrous K_2CO_3 (5.6 g, 41 mmol) was added into the 20 ml DMF solution of pyrocatechol (2.20 g, 20 mmol) at 100 °C. After 0.5 h, a solution of *N*-methyl-*N*-phenylchloroacetamide in 10 ml DMF was added dropwise to the mixture and maintained at 110 °C for 7 h. When cooled, 60 ml distilled water was poured and the turbid solution was extracted by 40 ml chloroform three times. Organic phase was washed with water and dried with anhydrous Na_2SO_4. Solvent removed, the residue was chromatographed to afford white solid (L) (yield: 82%).

2.3. General preparation of the complexes

A solution of 0.1 mmol lanthanide picrate in 5 ml anhydrous ethanol was added dropwise to a solution of L in 10 ml anhydrous ethanol. The mixture was stirred at room temperature for 5 h. The precipitated solid complex was filtered, washed with ethanol and dried in vacuo over P_4O_{10} for 2 days.

All the complexes are yellow powers and stable in air. Single crystals of the solvated terbium complex $[Tb(pic)_3L]\cdot 3MeCN$ were grown and recrystallized from MeCN with slow evaporation at room temperature. About a month later, transparent yellow crystals formed from the solution.

2.4. Chemical and physical measurements

The metal ions were determined by EDTA titration using xylenal orange as an indicator. C–H–N analysis was determined by using a Vario-EL analyzer. Conductivity was determined using a conductivity bridge with 10^{-3} mol cm^{-3} in MeOH at 25 °C. IR spectra were recorded on a Nicolet AVATAR 360 FT-IR instrument using KBr discs in the 400–4000 cm^{-1} region. ^{1}H NMR spectra were measured on a Brucker AM200 spectrometer in CD_3COCD_3 solution with TMS as internal standard.

2.5. X-ray crystallography

For the terbium complex, X-ray measurements were performed on a Siemens P4 four-circle diffractometer with graphite monochromatized Mo Kα radiation at 285(2) K. A summary of crystallographic data and details of the structure refinements are listed in Table 1. The structure was solved by direct methods and refined by full matrix least-squares techniques with all non-hydrogen atoms treated anisotropically. All calculations were performed with the program package SHELXTL.

Table 1
Crystal data and structure refinement for the complex $[Tb(pic)_3L]$

Empirical formula	$C_{48}H_{39}N_{14}O_{25}Tb$
Temperature (K)	285(2)
Formula weight	1370.85
Crystal size (mm)	$0.56 \times 0.48 \times 0.20$
Crystal system	triclinic
Space group	$P\bar{1}$
a (Å)	14.273(2)
b (Å)	14.955(2)
c (Å)	16.572(2)
α (°)	97.898(9)
β (°)	111.386(8)
γ (°)	113.090(7)
V (Å^3)	2862.9(7)
Z	2
D_{calc} (g cm^{-3})	1.590
$F(0\,0\,0)$	1380
Λ (Å)	0.71073
Reflections collected	10578
Independent reflections	9683
θ Range for data collection	1.57–25.01
Range of h, k, l	$0 \le h \le 16$ $-16 \le k \le 15$ $-19 \le l \le 18$
Gooding-of-fit on F^2	0.794
Final R indices $[I > 2\sigma(I)]$ [a]	$R_1 = 0.0363$, $wR_2 = 0.0563$
R indices (all data)	$R_1 = 0.0638$, $wR_2 = 0.0603$
Largest difference peak hole (e Å^{-3})	0.362, −0.419

[a] $w = 1/[\sigma^2(F_o^2)+(0.0337P)^2]$; $P = (F_o^2+F_c^2)/3$.

2.6. Solvent extraction

The multitracer solution was prepared by using gold foil as the target material irradiated with 60 MeV nucleon^{-1} $^{18}O^{8+}$ ion beam at the Heavy Ion Research Facility in Lanzhou, China. The chemical separation procedure was similar to that described in the literature [8]. The multitracer solution obtained contained nine radioactive rare earth nuclides: ^{141}Ce, ^{147}Eu, ^{149}Gd, ^{153}Tb, ^{160}Er, ^{167}Tm, ^{166}Yb, ^{177}Lu and ^{87}Y. The solvents were saturated with each other prior to use to prevent volume changes of the phases during extraction. Ion strength was adjusted to be 0.1 by a lithium chloride solution. An aqueous picric acid solution (2.0 cm^3) containing the required multitracer at pH 2.50 was vigorously shaken with an equal volume of the nitrobenzene solution of L in a test tube with a ground stopper at room temperature for 5 min. After phase separation by centrifugation (1 min, 3000 rpm), 1.0 cm^3 samples were taken from each phase and their γ-activities were assayed using of a calibrated HPGe γ-ray spectrometer. The detector has an efficiency of 40% and resolution of 2.3 keV at 1322 keV. The γ-ray spectra recorded on 4096 channels were analyzed and the peak areas were computed with the SAMPO [9] program. Assignment of the nuclides to each peak of the γ-ray spectra was made on the basis of its energy and half-life. The distribution ratio (D) was determined as a ratio of

Table 2
Analytical data and molar conductance values for [Ln(pic)$_3$L] (Ln = Gd, Tb, Er, Y)

Complex	C (%) found (calc.)	H (%) found (calc.)	N (%) found (calc.)	Ln (%) found (calc.)	Λm (s cm^2 mol^{-1})
Gd(pic)$_3$L	40.52(40.48)	2.71(2.43)	12.42(12.37)	12.62(12.52)	19.27
Tb(pic)$_3$L	40.45(40.43)	2.57(2.43)	12.32(12.45)	12.74(12.70)	16.58
Er(pic)$_3$L	40.19(40.16)	2.36(2.41)	12.52(12.27)	13.32(13.02)	18.33
Y(pic)$_3$L	42.82(42.83)	3.23(2.57)	13.08(13.09)	7.55(7.70)	16.52

the radioactive strengths of the organic and aqueous phases.

3. Result and discussion

Analytical data for the complexes (presented in Table 2) conform to a 1:3:1 metal-to-picrate-to-L stoichiometry. All complexes are soluble in DMSO, DMF, MeCN, methanol and acetone, and are slightly soluble in ethanol, chloroform and ethyl acetate. They are sparingly soluble in benzene, Et_2O and cyclohexane. The molar conductance values of the complexes in methanol (Table 2) indicate the presence of a non-electrolyte [10].

3.1. IR spectra

The IR spectrum of free L shows bands at 1677 and 1117 cm^{-1} assigned to ν(C=O) and ν(Ar–O–C). In the complexes, the bands shift by approximately 45 and 35 cm^{-1} towards lower wavenumbers, indicating that the C=O and ether O-atoms take part in coordination to the metal ions. The different shifts of the wavenumbers indicate that the Ln–O (carbonyl) bond is stronger than the Ln–O (ether) bond.

The OH out-of-plane bending vibration of free HPic at 1151 cm^{-1} disappears in the spectra of the complex, indicating that the H-atom of the OH group is replaced by Ln$^{(III)}$. The vibration ν(C–O) at 1265 cm^{-1} is shifted toward higher frequency by approximately 10 cm^{-1} in the complex. This is due to the following different effects. First, after forming the Ln–O bond, the π-bond character in the C–O bond increases. Secondly, coordination of the oxygen atom of L to Ln$^{(III)}$ causes the π-character to be weakened. The free HPic has $\nu_s(NO_2)$ at 1342 cm^{-1}, which splits into two band at approximately 1362 and 1329 cm^{-1}, respectively, in the complexes. This indicates that the nitronyl O-atoms take part in coordination [6].

3.2. ^{1}H NMR spectra

The ^{1}H NMR spectra of free L and its lanthanide complexes were measured in CD_3COCD_3. Upon coordination, the signals of –C(O)–CH– are shifted towards lower field by 0.42 ppm (from 4.46 to 4.88 ppm) and those of –C_6H_4– protons by only 0.09 ppm (from 6.85 to 6.94 ppm). This is probably due to the inductive effect of Ln–O (L) bands and a change in the conformation of the ligand in the complexes. The larger shift for –C(O)–CH– protons than for –C_6H_4– protons indicates that the Ln–O (C=O) bond is stronger than the Ln–O (Ar–O–C) bond [11].

The ^{1}H NMR signal of the OH group in free HPic disappears in the complexes, indicating that the H-atom of the OH group is replaced by Ln$^{(III)}$. The benzene ring protons of the free HPic exhibit a singlet at 9.12 ppm. Upon coordination, the signal moves to higher field, respectively, at 9.02 ppm. Only one singlet is observed for the benzene ring protons of the three coordination picrate groups indicating fast exchange among the group in solution [12].

3.3. X-ray crystal structure

Fig. 1 shows the structure and the atomic numbering schemes for the Tb$^{(III)}$ complex in [Tb(pic)$_3$L]·3MeCN. Selected bond lengths and angles are given in Table 3.

Table 3
Selected bond lengths (Å) and angles (°) for the Tb complex

Bond lengths			
Tb–O(1)	2.331(3)	Tb–O(2)	2.567(2)
Tb–O(3)	2.545(2)	Tb–O(4)	2.352(3)
Tb–O(5)	2.264(3)	Tb–O(12)	2.279(3)
Tb–O(18)	2.562(3)	Tb–O(19)	2.240(3)
Tb–O(25)	2.606(3)		
Bond angles			
O(1)–Tb–O(2)	63.60(9)	O(3)–Tb–O(18)	90.6(1)
O(1)–Tb–O(3)	124.19(9)	O(3)–Tb–O(19)	142.48(9)
O(1)–Tb–O(4)	158.41(9)	O(3)–Tb–O(25)	143.84(9)
O(1)–Tb–O(5)	80.8(1)	O(4)–Tb–O(5)	80.5(1)
O(1)–Tb–O(12)	87.8(1)	O(4)–Tb–O(12)	113.6(1)
O(1)–Tb–O(18)	130.5(1)	O(4)–Tb–O(18)	64.9(1)
O(1)–Tb–O(19)	85.0(1)	O(4)–Tb–O(19)	81.5(1)
O(1)–Tb–O(25)	66.2(1)	O(4)–Tb–O(25)	121.8(1)
O(2)–Tb–O(3)	60.60(8)	O(5)–Tb–O(12)	142.51(9)
O(2)–Tb–O(4)	119.77(9)	O(5)–Tb–O(18)	144.1(1)
O(2)–Tb–O(5)	72.18(9)	O(5)–Tb–O(19)	80.8(1)
O(2)–Tb–O(12)	70.77(9)	O(5)–Tb–O(25)	133.68(9)
O(2)–Tb–O(18)	133.03(9)	O(12)–Tb–O(18)	66.2(1)
O(2)–Tb–O(19)	140.97(9)	O(12)–Tb–O(19)	133.9(1)
O(2)–Tb–O(25)	115.88(9)	O(12)–Tb–O(25)	70.09(9)
O(3)–Tb–O(4)	63.07(9)	O(18)–Tb–O(19)	84.7(1)
O(3)–Tb–O(5)	81.58(9)	O(18)–Tb–O(25)	65.5(1)
O(3)–Tb–O(12)	75.60(9)	O(19)–Tb–O(25)	65.4(1)

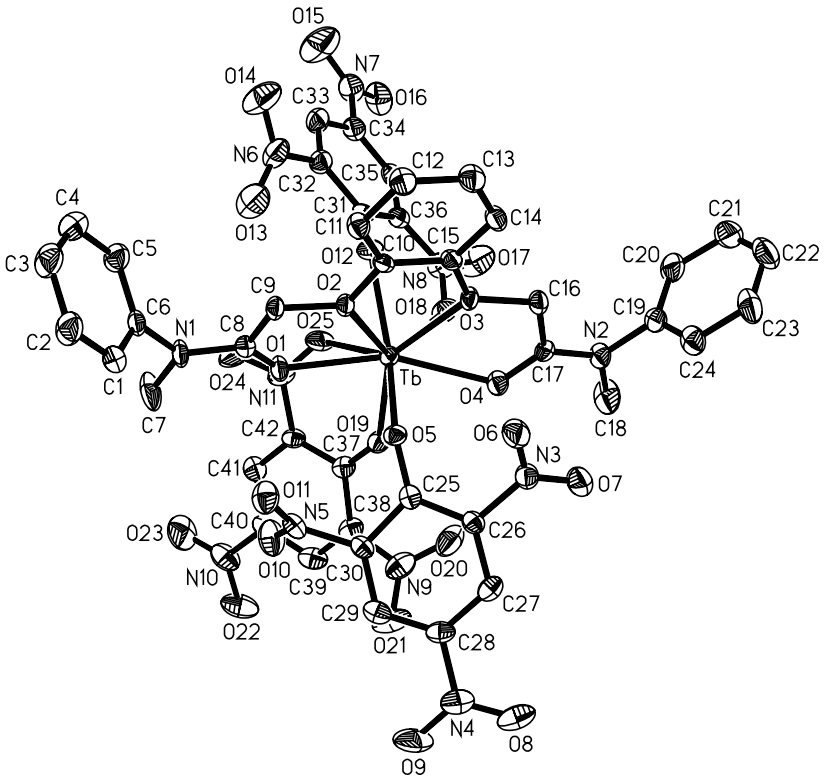

Fig. 1. Molecular structure of $[Tb(pic)_3L]$ with atom labeling scheme.

The crystal structure is composed of $[Tb(Pic)_3L]$ and $3CH_3CN$ linked by van der Waals' forces. $Tb^{(III)}$ ion is nona-coordinated by four oxygen atoms of L and five O-atoms of two bidentate and one unidentate picrates. The coordination polyhedron is a distorted mono-capped square anti-prism. Four O-atoms of L (O(1), O(2), O(3), O(4)) are not quite coplanar. Their deviation from the mean plane is in the range of 0.09–0.16 Å. The Tb atom lies out of this plane by 0.40 Å. The average distance between the $Tb^{(III)}$ ion and the coordination oxygen atoms is 2.416 Å, where the Tb–O(19) is the shortest, owing probably to the higher electron density on the oxygen anion of the picrate and the smaller steric effect. The Tb–O (C=O) distance (mean 2.342 Å) are significantly shorter than the Tb–O (Ar–O–C) distance (mean 2.556 Å), which suggests that the Tb–O (C=O) bond is stronger than the Tb–O (Ar–O–C) bond, in agreement with the ^1H NMR and IR spectral data.

3.4. Extracting data

Table 4 shows the distribution ratios and separation coefficients of the lanthanide ions for L. The data indicate that the sequence of the extractability of the

Table 4
The distribution ratios and separation coefficients of rare earth ions for L

	Ce	Eu	Gd	Tb	Er	Tm	Yb	Lu	Y
D	1.88	1.21	0.91	0.52	0.21	[a]	[a]	[a]	[a]
RE/Ce	–	0.64	0.48	0.28	0.11	[b]	[b]	[b]	[b]
RE/Eu	1.55	–	0.75	0.43	0.17	[b]	[b]	[b]	[b]
RE/Gd	2.07	1.33	–	0.57	0.23	[b]	[b]	[b]	[b]
RE/Tb	3.62	2.33	1.75	–	0.40	[b]	[b]	[b]	[b]
RE/Er	8.95	5.76	4.33	2.48	–	[b]	[b]	[b]	[b]
RE/Tm	[b]	[b]	[b]	[b]	[b]	–	[b]	[b]	[b]
RE/Yb	[b]	[b]	[b]	[b]	[b]	[b]	–	[b]	[b]
RE/Lu	[b]	[b]	[b]	[b]	[b]	[b]	[b]	–	[b]
RE/Y	[b]	[b]	[b]	[b]	[b]	[b]	[b]	[b]	–

Aqueous phase: [Hpic] = 0.02 mol l^{-1}, pH 2.50; organic phase: [L] = 5.0×10^{-4} mol l^{-1}; $T = 18$ °C.
[a] Very low *D* or no extraction.
[b] Unable to calculate.

rare earth ions for L is in an inversive order. This is because the extraction of lanthanide ions from the aqueous phase to the organic phase gets more difficult with increasing atomic number.

In conclusion, L, acting as a tetradentate ligand, can form stable solid complexes with lanthanide ions and exhibits a caverned conformation, which is suitable for the uptake of a cation. The internal cavity formed by the coordination oxygen atoms is sensitive to the variation of the lanthanide ions. In addition, the coordination stability also depends heavily on the ligand's terminal group.

4. Supplementary material

Crystallographic data for the structural analysis have been deposited with the Cambridge Crystallographic Data Center, CCDC No. 200308. Copies of this information may be obtained free of charge from the director, CCDC, 12 Union Road, Cambridge CB2 IEZ, UK (fax: +44-1223-336033; e-mail: deposit@ccdc.cam.ac.uk or www: http://www.ccdc.cam.ac.uk).

Acknowledgements

We are grateful to the National Natural Science Foundation of China (projects 29571014 and 20071015), the Foundation for University Key Teachers of the Ministry of Education, and a Key Project of the Ministry of Education of China (01170) for financial support.

References

[1] S.X. Liu, W.S. Liu, M.Y. Tan, K.B. Yu, G.Z. Tan, Helv. Chim. Acta 80 (1997) 586.
[2] L.Y. Fan, W.S. Liu, X.M. Gan, N. Tang, M.Y. Tan, W.H. Jiang, K.B. Yu, Polyhedron 19 (2000) 779.
[3] Y.S. Yang, Y.Z. Ding, G.Z. Tan, J.Z. Xu, Z.Q. Yiao, F.S. Zhang, J. Nucl. Radiochem. 6 (1984) 196.
[4] Y. Gao, J.Z. Ni, J. Nucl. Radiochem. 5 (1983) 146.
[5] Y. Yang, Y. Ding, J. Nucl. Radiochem. 4 (1982) 21.
[6] Y.C. Tian, Y.Q. Liang, J.Z. Ni, Chem. J. Chin. Univ. 9 (1988) 113.
[7] W. Zhang, H.W. Hu, Nanjing Daxue Xuebao 21 (1985) 662.
[8] X. Yin, J. Du, X. Zhang, X. Wang, X. Dai, T. Sun, Z. Tao, J. Radioanal. Nucl. Chem. Lett. 214 (1996) 89.
[9] J.T. Routti, S.G. Prussin, Nucl. Instrum. Methods 72 (1969) 125.
[10] W.J. Geary, Coord. Chem. Rev. 7 (1971) 81.
[11] S.X. Liu, W.S. Liu, M.Y. Tan, K.B. Yu, J. Coord. Chem. 10 (1996) 391.
[12] X. Mao, L.F. Shen, J.Z. Ni, Bopuxuezazhi 1 (1985) 201.